JOURNAL OF MATERIALS SCIENCE, 30 (1995) 932–937

Particle generation and film formation in an atmospheric-pressure chemical vapour deposition process using tetraethylorthosilicate

MOTOAKI ADACHI
Research Institute for Advanced Science and Technology, University of Osaka Prefecture, 1-2 Gakuen-cho, Sakai, Osaka 593, Japan

KIKUO OKUYAMA
Department of Chemical Engineering, Hiroshima University, 1-4-1 Kagamiyama, Higashi-Hiroshima, Hiroshima 724, Japan

NOBORU TOHGE
Department of Metallurgical Engineering, Kinki University, 3-4-1 Kowakae, Higashi-Osaka, Osaka 577, Japan

Effects of an oxygen flow rate on film formation and nanometre-sized particle generation in the gas phase were examined simultaneously in an atmospheric-pressure chemical vapour deposition reactor using tetraethylorthosilicate (TEOS). The critical temperature for particle generation decreased rapidly to 340 °C from 740 °C with increasing oxygen flow rate, but it decreased slightly to 600 °C from 700 °C for film formation. There were no conditions where film was deposited without particle generation in a TEOS/O_2 system. The nanometre-sized particles generated in the systems were amorphous and non-spherical, and their size distributions were polydisperse. The Fourier transform infrared (FT-IR) and thermal desorption (TDS) spectra of the particles were not affected by oxygen flow rate, and showed that the particles contained a small amount of an ethoxy group and a relatively large amount of a hydroxyl group. It was found from comparisons between FT-IR and TDS spectra of particles and films that the SiO_2 films were formed by β-elimination reactions, where C_2H_4 and H_2O are released from the ethoxy group.

1. Introduction

Silicon dioxide film deposited by an atmospheric-pressure chemical vapour deposition (APCVD) using tetraethylorthosilicate (TEOS) are used extensively in very-large-scale integration (VLSI) technology for constructing multilevel interconnection of deep submicron layers, because the film shows excellent step coverage. In a TEOS-CVD reactor, fine particles are often generated and may deposit on the films. As a result, the electrical characteristics of the films may be altered to the point of the failure of the microcircuits. Investigation of particle formation by gas-phase nucleation in the CVD reactor is therefore important for the development of a low-contamination TEOS-CVD process. In previous papers [1, 2], we reported conditions under which nanometre-sized particles were generated in a APCVD reactor using TEOS.

In this study, the effects of oxygen concentration on particle generation and film formation were examined. The size distribution and number concentration of particles generated during film formation were measured by means of aerosol sizing technique and the shape of the generated particles was observed using transmission electron microscopy (TEM). The particles and vapour generated in the reactor were further collected by the electrostatic particle collector and the vapour condenser, respectively. The particles, vapour and films thus captured were analysed by means of Fourier-transform infrared (FT-IR) and thermal desorption (TDS) spectroscopy.

2. Experimental method

The schematic diagram of the APCVD system used in this study in shown in Fig. 1. The system consisted of a TEOS evaporator, a CVD reactor, an electrostatic precipitator, and equipment for measuring particle size and number concentration. The reactor was a horizontal quartz tube with an inner diameter of 30 mm, and was heated by an infrared furnace where the length was 236 mm. Particle-free He gas was used as the carrier gas at a flow rate of 30 or 100 $cm^3 min^{-1}$. The He gas was passed through the TEOS evaporator where the liquid TEOS was kept at 0 °C. The vapour leaving the evaporator was saturated with TEOS. The TEOS/He vapour was then diluted with additional particle-free He gas and mixed with oxygen gas flowing at a flow rate of 30, 100 or

0022–2461

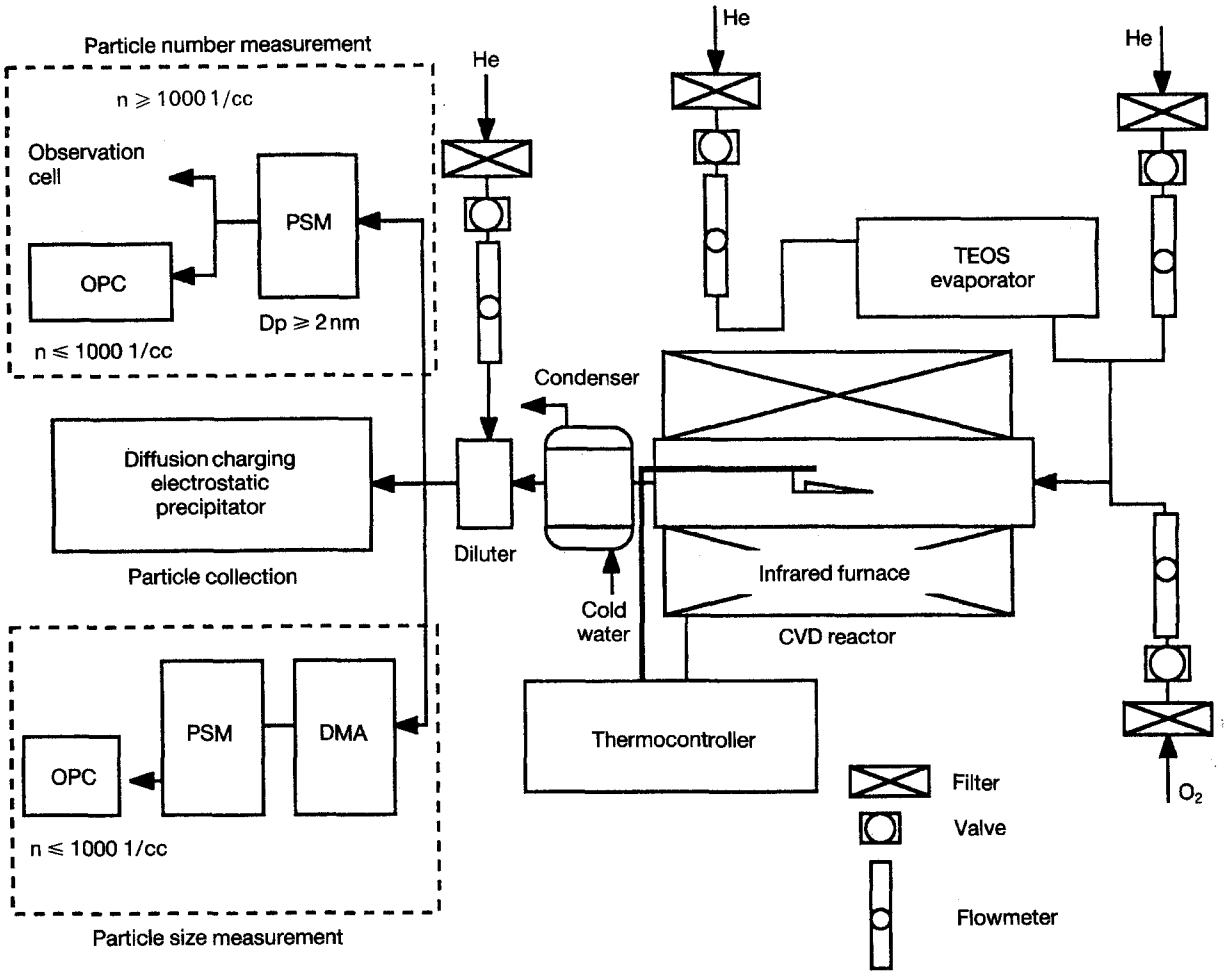

Figure 1 Schematic diagram of TEOS-atmospheric pressure CVD system.

200 $cm^3\ min^{-1}$. The $TEOS/O_2/He$ mixture was continuously fed into the reactor at a total flow rate of 400 $cm^3\ min^{-1}$.

In the reactor of 20×20 mm Si(100) wafer was placed on a quartz holder and tilted about 2° from horizontal. On the wafer a film was deposited to measure the FT-IR and TDS spectra and film growth rate. The vapours produced in the CVD reactor were deposited on the Si wafer placed in the vapour condenser to measure FT-IR and TDS spectra. The particles generated in the CVD reactor were first diluted with particle-free He gas at flow rate of 0.61 min^{-1} to prevent particle coagulation. They were then introduced to two particle-measuring systems or to an electrostatic particle collector [3]. For measuring size of generated particles, a differential mobility particle sizer (differential mobility analyser (DMA)/particle size magnifier (PSM)/optical particle counter (OPC; Rion KC-01B) set) [1, 2] was used. For the particle number concentration, the fine particles were enlarged in the PSM and the grown particles were counted with the OPC or by observing in an observation cell using a TV camera with He–Ne laser beam to illuminate individual aerosol particles [1]. For FT-IR and TDS spectroscopy, the particles were directly captured on the Si wafer in the electrostatic particle collector; for TEM observation, they were captured on a Cu mesh.

Infrared absorption spectra of the films, particles, and vapours were measured using an FT-IR spectrophotometer (Perkin-Elmer 1760X) and their TDS spectra were obtained using a TDS spectrometer (Denshi Kagaku EMD-WA1000). Film thickness was determined with an ellipsometer (Nanometrics AFT-210).

3. Results and discussion

Fig. 2 shows the particle number concentration and the growth rate of SiO_2 film in the APCVD reactor as a function of furnace temperature T_f, for TEOS/He and $TEOS/O_2/He$ systems. The TEOS concentrations C_{TEOS} were 2.66×10^{-6} and 5.55×10^{-7} $moll^{-1}$ and the oxygen flow rate was 100 $cm^3\ min^{-1}$. When the furnace temperature was raised from room temperature at $C_{TEOS} = 2.66 \times 10^{-6}$ $moll^{-1}$ particles suddenly appeared at $T_f = 740$ and 340 °C for TEOS/He and $TEOS/O_2/He$ systems, respectively. And, the particle number concentrations became constant values after rapidly increasing. The critical temperature for particle generation increased by 5–20 °C when TEOS concentration was decreased to 5.55×10^{-7} $moll^{-1}$. The particle number concentrations attained to constant values were changed with TEOS concentration. The film formation started at $T_f = 700$ and 600 °C for TEOS/He and $TEOS/O_2/He$ systems, respectively, when TEOS concentration was 2.66×10^{-6} $moll^{-1}$. And, the film growth rate increased with furnace temperature and TEOS concentration. From

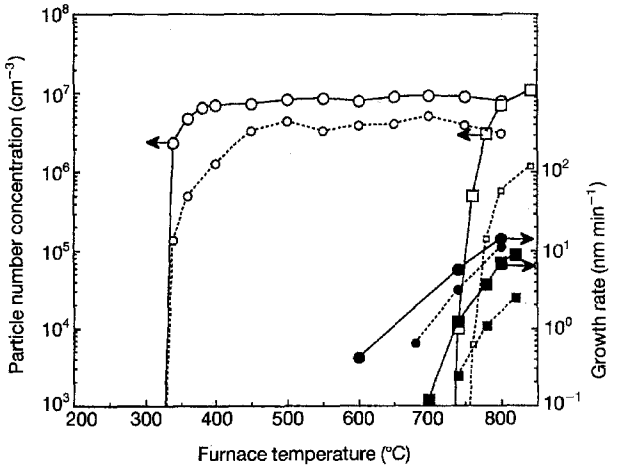

Figure 2 Particle number concentration and film growth rate at two TEOS concentrations, $C_{TEOS} = 5.5 \times 10^{-7}$ (...□.., ■.. TEOS/He; ...○, .●.., TEOS/O_2/He) and 2.66×10^{-6} mol l^{-1} (—□—, —■—, TEOS/He; —○—, —●—, TEOS/O_2/He) as a function of furnace temperature for the TEOS/He and TEOS/O_2/He systems.

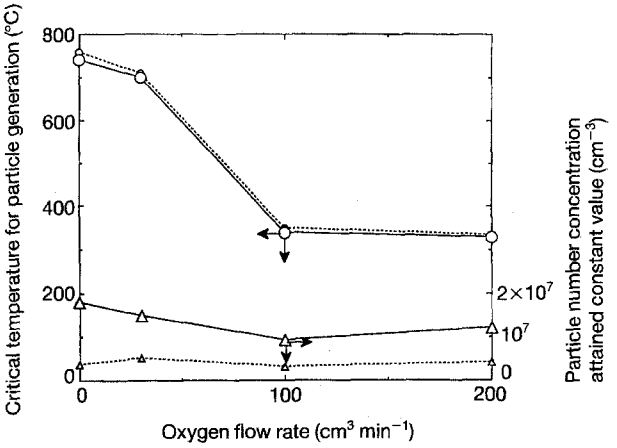

Figure 3 Critical temperature for particle generation and particle number concentration attained constant value as a function of oxygen flow rate for TEOS/O_2/He system with two TEOS concentrations, $C_{TEOS} = 5.5 \times 10^{-7}$ (----○----, ----▲----) and 2.66×10^{-6} mol l^{-1} (—○—, —△—).

comparisons between critical temperatures for particle generation and film formation in TEOS/He system, the films were prepared without particle generation in temperature ranges of 700–740 °C and 740–760 °C with $C_{TEOS} = 2.66 \times 10^{-6}$ and 5.55×10^{-7} mol l^{-1}, respectively. For TEOS/O_2/He system, on the other hand, particles were generated at furnace temperatures lower than the critical temperature for film formation. The above results suggest that the film formation without particle generation is possible in an APCVD reactor using TEOS/He system, but is not in the reactor using the TEOS/O_2/He system.

In order to make clear the effect of oxygen on the particle generation, the experiments for particle generation were carried under various oxygen flow rates. The critical temperature for particle generation (T_c) and the particle number concentrations reached to constant values (n_c) were shown in Fig. 3 as a function of the oxygen flow rate. For both TEOS concentrations of $C_{TEOS} = 2.66 \times 10^{-6}$ and 5.55×10^{-7} mol l^{-1}, the critical temperature decreased with oxygen flow rate in the range of $Q_{O2} = 0$–100 cm^3 min^{-1} and attained to constant values at $Q_{O2} \geq 100$ cm^3 min^{-1}. The particle number concentrations which reached to constant values at a high furnace temperature were independent of the oxygen flow rate and depended on only the TEOS concentration.

Fig. 4 shows the size distributions of particles generated at the oxygen flow rate of $Q_{O2} = 0$, 30, and 100 cm^3 min^{-1}. The particles were prepared at $T_f = 780$, 740 and 340 °C with $C_{TEOS} = 2.66 \times 10^{-6}$ mol l^{-1} at $Q_{O2} = 0$, 30, and 100 cm^3 min^{-1}, respectively. At these temperatures, about 3×10^6 particles/cm^{-3} were generated. Three particle size distributions were lognormal. The size distribution at $Q_{O2} = 0$ cm^3 min^{-1}, i.e. the TEOS/He system, was monodisperse of which the geometric standard deviation σ_g was 1.32, but that at $Q_{O2} = 100$ cm^3 min^{-1} was polydisperse of $\sigma_g = 1.42$. The geometric mean diameter D_{pg} for $Q_{O2} = 0$ cm^3 min^{-1} was larger than that for $Q_{O2} = 100$ cm^3 min^{-1}. The values of the

Key	System	Q_{O2} (cm^3 min^{-1})	D_{pg} (nm)	σ_g
□	TEOS/He	0	37.5	1.32
○	TEOS/O_2/He	30	38.0	1.45
○	TEOS/O_2/He	100	25.8	1.42

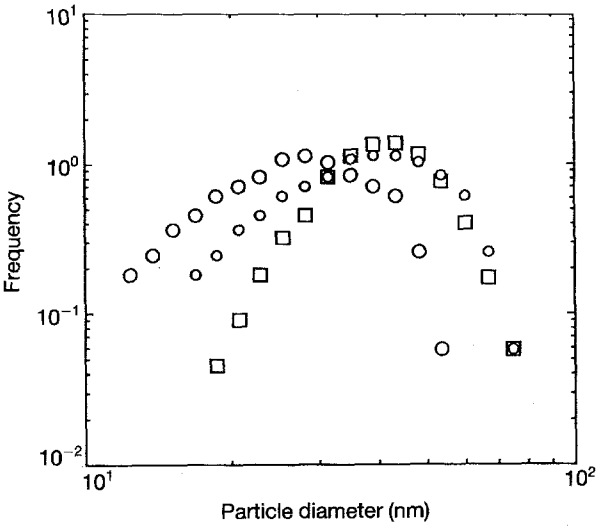

Figure 4 Particle size distributions generated at three oxygen flow rates, $Q_{O2} = 0$ cm^3 min^{-1} in TEOS/He system and $Q_{O2} = 30$ and 100 cm^3 min^{-1} in TEOS/O_2/He system.

geometric mean diameter and the geometric standard deviation for $Q_{O2} = 30$ cm^3 min^{-1} were nearly equal to $D_{pg} = 37.5$ nm for $Q_{O2} = 0$ cm^3 min^{-1} and $\sigma_g = 1.42$ for $Q_{O2} = 100$ cm^3 min^{-1}, respectively.

Transmission electron micrographs of the particles are shown in Fig. 5. The particles produced with the TEOS/He system ($Q_{O2} = 0$ cm^3 min^{-1}) were spherical, but those with the TEOS/O_2/He system at $Q_{O2} = 30$ and 100 cm^3 min^{-1} were non-spherical. Electron diffraction photographs of the particles indicated that they were amorphous.

The difference in the shape and size distribution of the particles suggests that the particle generation mechanism of the TEOS/He system is different from that of the TEOS/O_2/He system. The gas-phase

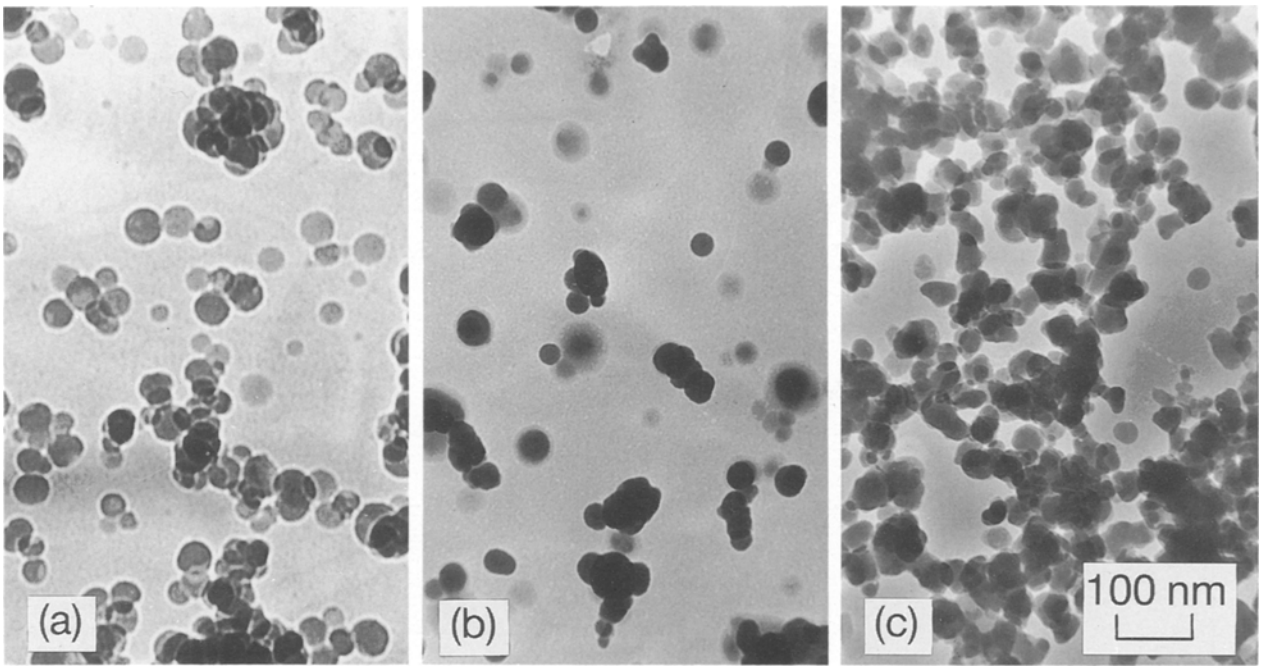

Figure 5 Transmission electron micrographs of ultrafine particles produced at $C_{TEOS} = 2.66 \times 10^{-6}$ mol l^{-1}; (a) $Q_{O2} = 0$ cm^3 min^{-1} in TEOS/He system, (b) $Q_{O2} = 30$ cm^3 min^{-1}, and (c) $Q_{O2} = 100$ cm^3 min^{-1} in TEOS/O_2/He system.

nucleation in the APCVD reactor is generally expected as follows [3]. In the rector, TEOS vapour is thermally decomposed or oxidized to produce supersaturated intermediates. If this supersaturation of the intermediates reaches a sufficient level, nanometre-sized primary particles are produced by homogeneous nucleation. When a large amount of primary particles are generated, larger secondary particles are formed mainly by the Brownian coagulation. On the other hand, when a small amount of primary particles are generated, particles grow mainly by heterogeneous condensation of the intermediates on the primary particles. Therefore, the monodispersity and spherical shape of the particles for TEOS/He system indicate that the particles grow by condensation of an intermediate on primary particles, which were a few nanometres in diameter. On the other hand, the polydispersity and non-spherical shape of the particles generated with the TEOS/O_2/He system indicate that particle growth is due to Brownian coagulation of nanometre-sized primary particles which are mass produced.

Fig. 6 shows the critical temperature of particle generation as a function of TEOS concentration for TEOS/He and TEOS/O_2/He systems. For the TEOS/O_2/He system, the critical temperature kept constant at about 340 and 710 °C with TEOS concentration at $Q_{O2} = 100$ and 30 cm^3 min^{-1}, respectively. On the other hand, it decreased slightly with TEOS concentration for TEOS/He system. Three solid curves mean that the particles are generated in the upper sides of these curves, but not in the under sides.

The FT-IR spectra of films, vapour, and particles are shown in Figs. 7(a) and (b) for TEOS/He and TEOS/O_2/He systems, respectively. The films, vapour, and particles were simultaneously prepared at $T_f = 740$ °C and $C_{TEOS} = 2.66 \times 10^{-6}$ mol l^{-1}. Solid, dotted, and fine curves in Fig. 7 show spectra for films,

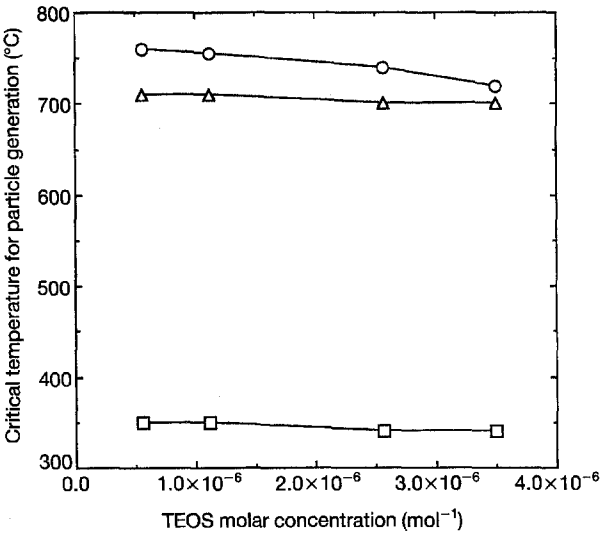

Figure 6 Critical temperature for particle generation as a function of TEOS concentration for three oxygen flow rates, $Q_{O2} = 0$ cm^3 min^{-1} in TEOS/He system (—○—) and $Q_{O2} = 30$ (—△—) and 100 cm^3 min^{-1} (—□—) in TEOS/O_2/He system.

vapours and particles, respectively. For films, the two spectra have the same absorption peaks. The dominant absorption peak around 1100 cm^{-1} is associated with the stretching motion of a Si–O bond. The absorption bands at 800 cm^{-1} and 470 cm^{-1} correspond to the deformation vibration of Si–O and Si–O–Si bonds, respectively. These spectra do not show evidence of OH or Si–OH bonds. For the particles, both spectra with TEOS/He and TEOS/O_2/He systems contain the weak absorption band at 940 cm^{-1} due to a Si–OH bond and the broad band at 3700 to 3100 cm^{-1} due to an O–H bond in addition to the bands at 1100, 800 and 470 cm^{-1}. The band near 610 cm^{-1} has been attributed to silica ring structures reported by Galeener [4]. Two spectra for the

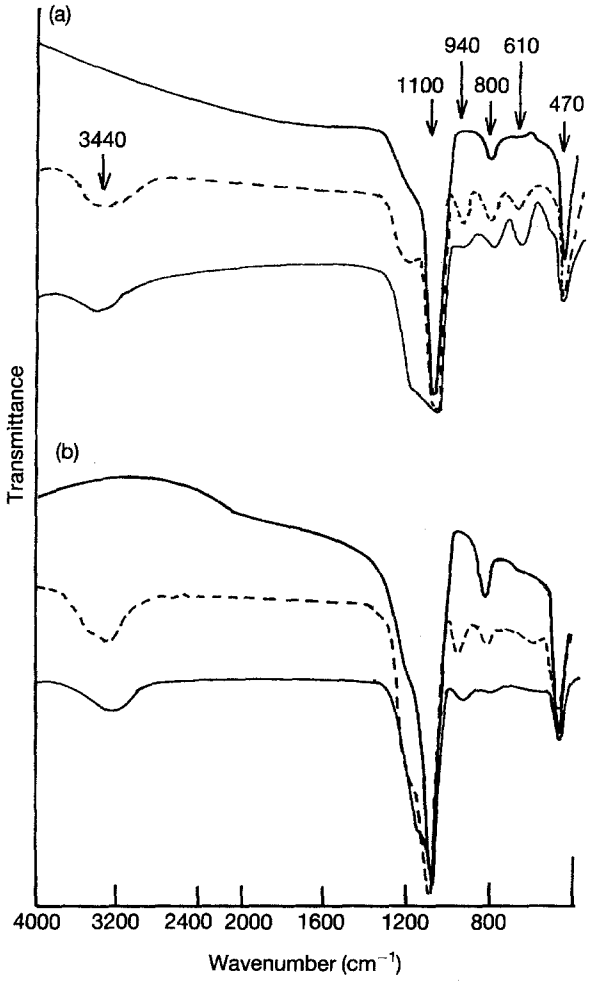

Figure 7 Fourier-transform infrared (FT-IR) spectra of film (solid curves), vapours (dotted curves) and particles (fine curves) generated at $T_f = 740\,°C$ and $C_{TEOS} = 2.66 \times 10^{-6}\,mol\,l^{-1}$; (a) in TEOS/He system and (b) in TEOS/O_2/He system with $Q_{O2} = 100\,cm^3\,min^{-1}$.

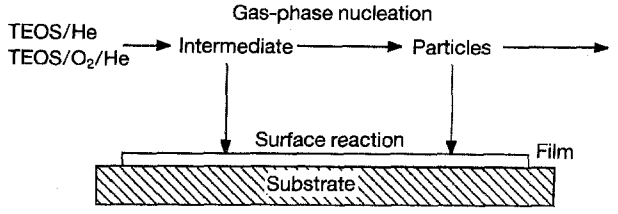

Figure 8 Particle and film formation in TEOS-APCVD reactor.

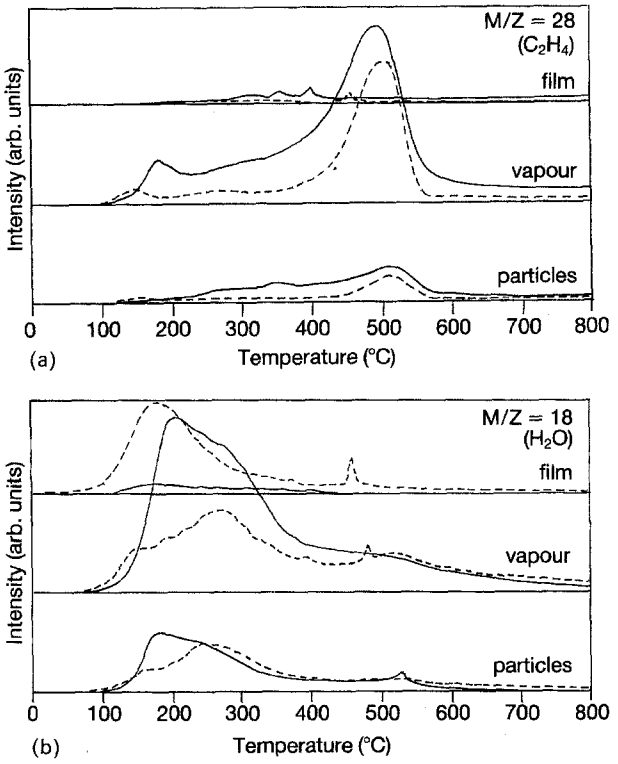

Figure 9 (a) Thermal desorption (TDS) spectra of C_2H_4 (M/Z = 28) for film, vapours and particles generated at $T_f = 740\,°C$ and $C_{TEOS} = 2.66 \times 10^{-6}\,mol\,l^{-1}$ in TEOS/He system (solid curves) and TEOS/O_2/He system (dotted curves) with $Q_{O2} = 100\,cm^3\,min^{-1}$. (b) Thermal desorption (TDS) spectra of H_2O (M/Z = 18) for film, vapours and particles generated at $T_f = 740\,°C$ and $C_{TEOS} = 2.66 \times 10^{-6}\,mol\,l^{-1}$ in TEOS/He system (solid curves) and TEOS/O_2/He system (dotted curves) with $Q_{O2} = 100\,cm^3\,min^{-1}$.

vapours show the same absorption peaks as the spectra for the particles. The peak at 1200 cm^{-1} in the spectrum for the vapours of the TEOS/He system was same as a shoulder of the dominant peak at 1100 cm^{-1} in other spectra. The identity of the peak has not been clarified. For both chemical systems, the agreements in the FT-IR spectra between the particles and the vapour suggests that the particles and the vapour are composed of same gas-phase intermediates. And, the agreement in the FT-IR spectra between the products with TEOS/He and TEOS/O_2/He systems means that FT-IR spectra cannot detect differences in the structure between the intermediates generated in these chemical systems.

From the agreement in the FT-IR spectra of the particles and the vapour, we thought the scheme of film formation and particle generation that occur in the TEOS-CVD reactor were as shown in Fig. 8. In the reactor TEOS vapour is thermally decomposed or oxidized to produce intermediates in the gas phase. The intermediates deposit on the wafer and are subjected to surface reaction to form a silicon dioxide film. Simultaneously, the gas-phase intermediate species nucleate to form particles. The particles and remaining intermediates are drawn out of the reactor. The intermediates are condensed in the vapour condenser and become liquid. The residence time of these gas-phase products is 25 s. On the other hand, the films are kept in the reactor for 20–50 min. Therefore, the difference in the FT-IR spectra between the films and the gas-phase products can be attributed to surface reactions occurring on the films during this longer time period.

We measured their thermal deposition spectra to examine the surface reaction. Figs 9(a) and (b) show the TDS spectra of mass fragments of 28(C_2H_4) and 18(H_2O) M/Z from the films, vapours and particles respectively, with TEOS/He and TEOS/O_2/He systems. The films, vapours, and particles were prepared at $T_f = 740\,°C$ and $C_{TEOS} = 2.66 \times 10^{-6}\,mol\,l^{-1}$ with both systems. Solid and dotted curves show spectra for TEOS/He and TEOS/O_2/He systems, respectively. In the spectra for C_2H_4 shown in Fig. 9(a), both vapours generated in the TEOS/He and TEOS/O_2/He systems have two peaks at 150–170 °C

and around 500 °C. The peak at 150–170 °C is associated with N_2 gas used during the TDS measurement. The one at around 500 °C is assigned to C_2H_4 generation from an ethoxy group (C_2H_5O–). Two spectra for the particles also have a peak at around 500 °C. In two spectra for the films, on the other hand, this peak does not appear. In the spectra for H_2O shown in Fig. 9(b), vapours and particles formed with TEOS/He and TEOS/O_2/He systems have two peaks at 150–300 °C and around 500 °C. The peak at 150–300 °C corresponds to desorption of H_2O which is adsorbed on the particles and vapours. The one at around 500 °C is associated with H_2O which is produced from an ethoxy group by a β-elimination reaction. In the spectra for films the peak is at the lower temperature only.

From the results of the TDS spectra, where the C_2H_4 was released, and results of the FT-IR spectra, where the absorption peak associated with the ethoxy group was not observed, the particles were found to be made up of intermediates that contain a small amount of an ethoxy group and a relatively large amount of a hydroxyl group. Intermediate species produced in the gas phase of the TEOS-APCVD reactor, therefore, also consist of these intermediates having a lower molecular weight than that of the generated particles. From the results of TDS spectra where the particles and the vapours release C_2H_4 and H_2O, these intermediates deposited on the substrate are found to form an SiO_2 layer by β-elimination reaction, where C_2H_4 and H_2O are released. This fact agrees with other reports of C_2H_4 being a major product in the TEOS-LPCVD reactor [5, 6].

4. Conclusion

The formation mechanisms of films and nanometre-sized particles in the APCVD reactor using TEOS/He and TEOS/O_2/He systems are as follows. In the gas phase, the intermediates that contain a small amount of an ethoxy group and a relatively large amount of a hydroxyl group are produced. On the substrate, at a furnace temperature higher than 500 °C, the intermediates deposit and form an SiO_2 layer by β-elimination reaction, where C_2H_4 and H_2O are released. Nanometre-sized particles are simultaneously generated in the gas phase by homogeneous nucleation of the intermediate and quickly drown out from the reactor. Then they contain ethoxy and hydroxyl groups.

Acknowledgements

We would like to thank J. Sato and M. Muroyama in SONY Co. for TDS measurement. This work was supported by three grants from the Mazda Foundation, the CVD Project Research of The Society of Chemical Engineers, Japan and the Ministry of Education, Culture and Science of Japan.

References

1. M. ADACHI, K. OKUYAMA, N. TOHGE, M. SHIMADA, J. SATO and M. MUROYAMA, *Jpn. J. Appl. Phys.* **31** (1992) L1439.
2. M. ADACHI, K. OKUYAMA, N. TOHGE, M. SHIMADA, J. SATO and M. MUROYAMA, *Jpn. J. Appl. Phys.* **32** (1993) L748.
3. K. OKUYAMA, Y. KOUSAKA, N. TOHGE, S. YAMAMOTO, J. J. WU, R. C. FLAGAN and J. H. SEINFELD, *AIChE J.* **32** (1986) 2010.
4. F. L. GALEENER, *J. Non-Cryst. Solids* **49** (1982) 53.
5. S. B. DESU, *J. Am. Ceram. Soc.* **72** (1989) 1615.
6. L. L. TEDDER, L. GUANGQUAN and J. E. CROWELL, *J. Appl. Phys.* **69** (1991) 7037.

Received 16 November 1993
and accepted 5 July 1994